(2)

OFFICE OF NAVAL RESEARCH

Contract No. N00014-91-J-1409

Technical Report No. 108

In-Situ Scanning Tunneling Microscopy as a Probe of Adsorbate-Induced Reconstruction at Ordered Monocrystalline Electrodes: CO on Pt(100)

by

C.M. Vitus, S.-C. Chang, B.C. Schardt, and M.J. Weaver

Prepared for Publication

in the

Journal of Physical Chemistry

Purdue University

Department of Chemistry

West Lafayette, Indiana 47907

October 1991

SECUPITY CLASSIFICATION OF THIS PAGE

REPORT DOCUMENTATION PAGE

Form Approved
OMB No 0704 0188

1a. REPORT SECURITY CLASSIFICATION Unclassified	1b. RESTRICTIVE MARKINGS
2a. SECURITY CLASSIFICATION AUTHORITY	3. DISTRIBUTION/AVAILABILITY OF REPORT Approved for public release and sale; its distribution is unlimited.
2b. DECLASSIFICATION/DOWNGRADING SCHEDULE	
4. PERFORMING ORGANIZATION REPORT NUMBER(S) Technical Report No. 108	5. MONITORING ORGANIZATION REPORT NUMBER(S)
6a. NAME OF PERFORMING ORGANIZATION Purdue University Department of Chemistry 6b. OFFICE SYMBOL (If applicable)	7a. NAME OF MONITORING ORGANIZATION Division of Sponsored Programs Purdue Research Foundation
6c. ADDRESS (City, State, and ZIP Code) Purdue University Department of Chemistry West Lafayette, IN 47907-1393	7b. ADDRESS (City, State, and ZIP Code) Purdue University West Lafayette, IN 47907
8a. NAME OF FUNDING/SPONSORING ORGANIZATION Office of Naval Research 8b. OFFICE SYMBOL (If applicable)	9. PROCUREMENT INSTRUMENT IDENTIFICATION NUMBER Contract No. N00014-91-J-1409
8c. ADDRESS (City, State, and ZIP Code) 800 N. Quincy Street Arlington, VA 22217	10. SOURCE OF FUNDING NUMBERS PROGRAM ELEMENT NO. / PROJECT NO. / TASK NO / WORK UNIT ACCESSION NO

11. TITLE (Include Security Classification)
In-Situ Scanning Tunneling Microscopy as a Probe of Adsorbate-Induced Reconstruction at Ordered Monocrystalline Electrodes: CO on Pt(100)

12. PERSONAL AUTHOR(S)
C.M. Vitus, S.-C. Chang, B.C. Schardt, and M.J. Weaver

13a. TYPE OF REPORT	13b. TIME COVERED	14. DATE OF REPORT (Year, Month, Day)	15. PAGE COUNT
Technical	FROM _____ TO _____	October 31, 1991	

16. SUPPLEMENTARY NOTATION

17. COSATI CODES			18. SUBJECT TERMS (Continue on reverse if necessary and identify by block number)
FIELD	GROUP	SUB-GROUP	in-situ scanning tunneling microscopy, atomic-level structure of ordered Pt(100) electrodes, iodine adlayers

19. ABSTRACT (Continue on reverse if necessary and identify by block number)

The atomic-level structure of ordered Pt(100) electrodes prepared by air-hydrogen flame annealing followed by iodine dosing and solution-phase replacement by CO has been examined by in-situ scanning tunneling microscopy. While large (1 x 1) substrate terraces are discernable in the presence of iodine adlayers, subsequent CO adsorption in 0.1 M $HClO_4$ yields dense arrays of smaller, 20–40Å, (1 x 1) islands. These domains coalesce upon positive alterations in the electrode potential. Parallel in-situ infrared spectroscopic measurements shows that these structural changes are accompanied by an attenuation of bridge-bound CO in the close-packed adlayer structure. The bridging CO is speculated to be present at the edges of the (1 x 1) domains, contained within which are predominantly atop coordinated CO.

20. DISTRIBUTION/AVAILABILITY OF ABSTRACT	21. ABSTRACT SECURITY CLASSIFICATION
☐ UNCLASSIFIED/UNLIMITED ☐ SAME AS RPT. ☐ DTIC USERS	
22a NAME OF RESPONSIBLE INDIVIDUAL	22b. TELEPHONE (Include Area Code) / 22c OFFICE SYMBOL

DD Form 1473, JUN 86 *Previous editions are obsolete.* SECURITY CLASSIFICATION OF THIS PAGE

ABSTRACT

The atomic-level structure of ordered Pt(100) electrodes prepared by air-hydrogen flame annealing followed by iodine dosing and solution-phase replacement by CO has been examined by in-situ scanning tunneling microscopy. While large (1 x 1) substrate terraces are discernable in the presence of iodine adlayers, subsequent CO adsorption in 0.1 M $HClO_4$ yields dense arrays of smaller, 20-40Å, (1 x 1) islands. These domains coalesce upon positive alterations in the electrode potential. Parallel in-situ infrared spectroscopic measurements shows that these structural changes are accompanied by an attenuation of bridge-bound CO in the close-packed adlayer structure. The bridging CO is speculated to be present at the edges of the (1 x 1) domains, contained within which are predominantly atop coordinated CO.

Scanning tunneling microscopy (STM) is currently developing rapidly as an in-situ real-space structural probe of metal-solution and other electrochemical interfaces. While only a few studies published so far achieve true atomic resolution of the substrate lattice or adlayers,[1-3] a number of reports attest to the ability of STM to image monoatomic steps and larger-scale substrate morphological features (for example, see refs. 4-6). Most work of the latter type has focussed on the effects of anodic oxide formation and removal on the substrate topology.[5,6] These results also suggest the prospect of utilizing STM to follow reconstruction of the surface atomic lattice as engendered by simple molecular and ionic adsorbates. Such adsorbate-induced surface reconstruction is a well-known, yet not entirely understood, phenomenon at single-crystal surfaces in ultrahigh vacuum (uhv) environments.[7]

A particularly interesting and widely-studied example is Pt(100). Clean Pt(100) reconstructs in uhv at temperatures below 1070K to yield a so-called "hex" [quasi-hexagonal (5 x 20)] phase, resembling a corrugated Pt(111) surface. The reconstruction can be lifted entirely by a number of adsorbates, such as CO and NO, to form the (1 x 1) surface lattice.[9,10] This process, induced by CO, has been followed in uhv by means of STM.[11] Infrared reflection-absorption spectroscopy (IRAS) has also been utilized recently to discern coverage-dependent details of CO and NO adlayer structures formed on initially hex and (1 x 1) Pt(100) surfaces.[12] These STM and IRAS data, as well as earlier low-energy energy diffraction (LEED) results,[10b] indicate that the CO-induced reconstruction results in the formation of local (1 x 1) domains on Pt(100).

The richness of the observed reconstruction behavior of Pt(100) in uhv earmarks this surface as an interesting candidate for exploring possible related phenomena in electrochemical systems. As for other platinum low-index faces, flame-annealing methods developed by Clavilier[13] and Wieckowski et al[14] are available by which ordered surfaces can readily be prepared in ambient

environments for electrochemical use. The latter approach involves the gas-phase formation of a protective iodine adlayer which can be removed subsequently by CO adsorption.[14] Atomic-resolution STM images of the iodine adlayers on Pt and Rh low-index faces, including Pt(100) (see below), indicate the well-ordered nature of surfaces formed in this manner.[1,15,16] This same pretreatment procedure has recently been utilized to prepare ordered low-index platinum and rhodium electrodes, including Pt(100),[17] on which the adsorption and electrooxidation of CO has been studied in detail by using in-situ IRAS.[17-22] Recently, atomic-resolution STM images of saturated CO adlayers on some of these non-reconstructed surfaces have also been obtained, initially on Pt(111),[16a] Rh(111),[3] and Rh(110).[23] Comparison with corresponding in-situ IRAS data affords CO adlayer structures with a level of atomic-level detail unprecedented for electrochemical systems.[3,23]

We report here in-situ STM data, including atomic-resolution images, of ordered Pt(100) surfaces in 0.1 M $HClO_4$. The replacement of iodine adlayers by CO is followed by means of STM. In particular, CO adsorption on Pt(100) is found to yield arrays of small, ca 20-40Å, (1 x 1) domains which exhibit potential-dependent morphologies. These images are combined with corresponding IRAS data to yield a picture of CO-induced reconstruction at the Pt(100)-aqueous interface.

EXPERIMENTAL SECTION

The Pt(100) single crystal (9 mm diameter, 2 mm thick) was obtained from Johnson Matthey; it was oriented within 1°. Laue x-ray back diffraction was used both to verify this crystallographic orientation and to determine the direction of the Pt rows on the exposed crystal face. The latter could be reproduced accurately with respect to the STM scan direction by means of a ledge milled into the back face of the crystal, mated with a groove machined in the microscope base. Two related surface pretreatments were employed. Method I followed essentially that of Wieckowski et al.[14] This entailed annealing the crystal to

redness for 1 min in an air–hydrogen flame, and cooling for 1.5 min in a N_2 stream approximately 2 cm over an iodine crystal. The protective iodine monolayer thus formed can be removed in 0.1 M $HClO_4$ at −0.25 V vs saturated calomel electrode (SCE) by bubbling in CO and solution flushing (vide infra). The CO adlayer can be removed subsequently by electrooxidation. Method II involved flame annealing as before, but cooling in nitrogen for 1 min before immersing in ultrapure water. The voltammograms obtained in 0.1 M $HClO_4$ after Method I were more indicative of a clean well-ordered surface (cf refs. 17, 20b); the charge under the hydrogen peak obtained with Method II is significantly smaller, suggestive of an influence from surface impurities.

Most experimental details of the STM measurements have been noted previously.[1,15,24,25] The microscope is a commercial Nanoscope II instrument with a bipotentiostat (Digital Instruments, Inc.) for in-situ electrochemical STM. The tip potential is held at virtual ground. As before,[1,3] variations in the substrate (working electrode) potential, E_{we}, were accompanied by parallel variations in the tip potential, E_{tip}, so that the surface–tip bias voltage, V_b, remains fixed. The V_b values selected were from −500 to 200 mV; the tip set-point currents, i_t, varied from 1 to 15 nA (see figure captions for specific values). The atomic-resolution STM images were obtained by using the "constant-height" mode. The larger-scale terrace images were obtained in a "topographic mode" at a slower scan rate, and were filtered to compensate for "surface tilt". The atomic-scale images were filtered where necessary by using a 2d-FT program in the Nanoscope software, being careful to avoid suppressing any significant imaging features.

The STM electrochemical cell holder, machined from Kel-F, contains the reference and counter electrode connections and is secured to the base by two set screws. The cell, made from Teflon, is sealed to the substrate surface via the electrode mount. The cell and holder were cleaned prior to each experiment using

hot Chromerge, and rinsed with ultrapure water. The counter electrode was a platinum wire. Two types of quasi-reference electrodes were employed: a chloride-coated silver wire, prepared as in ref. 26, or an oxidized gold wire prepared by anodizing at 3.0 V (vs Pt wire) in 0.1 M $HClO_4$. The STM tips were made from 0.010 in. tungsten wire electrochemically etched to a sharp point in 1 M KOH, and insulated with clear nail polish ("Wet 'n Wild", Pavion Ltd.).

Details of the electrochemical IRAS measurements are largely as described earlier.[20] The FTIR spectrometer is an IBM/Bruker IR-98 instrument with a Globar light source and a MCT narrow-band detector. Carbon monoxide (99.8%) was from Matheson, and perchloric acid (double distilled) from G.F. Smith Chemicals. Ultrapure water was obtained using a Milli-Q system (Millipore, Inc.). All electrode potentials reported here are on the SCE scale.

RESULTS

Atomic-resolution STM images of iodine-covered Pt(100) surfaces prepared by either Methods I or II exhibited large (ca 50 nm) terraces containing ordered iodine adlayer domains. The adlayers resulting from gas-phase iodine dosing as in Method I have the symmetry $c(\sqrt{2} \times 5\sqrt{2})R45°$ (iodine coverage, $\theta_I = 0.6$).[27] Immersing surfaces prepared by Method II into solutions of 1 mM KI + 0.1 M $HClO_4$ also yielded well-ordered iodine adlayers, with symmetry $(\sqrt{2} \times \sqrt{2})R45°$ ($\theta_I = 0.5$), as discerned from STM images obtained either in air or in 0.1 M $HClO_4$ under potential control. Figure 1 displays a typical atomic-resolution in-situ STM image of iodine-coated Pt(100), prepared by Method I, in 0.1 M $HClO_4$ at 0.25 V vs SCE. A $c(\sqrt{2} \times 5\sqrt{2})R45°$ adlayer symmetry can be deduced given that the direction of the Pt(100) substrate rows is known from the Laue x-ray diffraction (vide supra); these rows run at -2° (and 88°) to the x-direction of the tip scan (corresponding to the x-axis of the images shown here). The symmetry properties of these adlattices strongly suggest that the underlying Pt(100) surface is present as correspondingly large (1 x 1) domains, rather than in the

"hex" or other reconstructed forms. Further evidence that such unreconstructed Pt(100) domains are actually present could be obtained under some conditions by the observation of (1 x 1) substrate images even in the presence of iodine adlayers. Such an atomic-resolution STM image, obtained in air, is shown in Fig. 2. The square-planar (100) lattice, with Pt-Pt distances of 2.7-2.8Å as expected, is clearly evident. Similar images could be obtained throughout a given (ca 50 nm size) substrate terrace region. A ($\sqrt{2}$ x $\sqrt{2}$)R45°-I adlayer image could be observed within the same surface region by lowering the set-point current from 15 to 0.2 nA at the same bias voltage as in Fig. 2, 50 mV. The observation of substrate STM images in the presence of iodine adlattices has been noted previously for Pt(111);[1] while the physical factors favoring the occurrence of substrate rather than adlayer images are somewhat unclear at present,[1] the phenomenon clearly is useful from an analytical standpoint.

Of central interest here is the effect of CO adsorption on the Pt(100) substrate morphology. Replacement of the iodine adlayer by CO in 0.1 M $HClO_4$ (constituting the final phase of the Method I pretreatment) yielded markedly different in-situ STM images. Figure 3A shows a typical image obtained at an electrode potential of -0.25 V vs SCE in 0.1 M $HClO_4$ containing near-saturated (ca 1 mM) CO. Specifically, the procedure entailed transferring the iodine-coated surface prepared by Method I to the STM cell, and replacing the iodine with adsorbed CO at -0.25 V by pipeting in CO-saturated 0.1 M $HClO_4$, flushing the cell, and repeating twice so as to expel residual solution-phase iodine.

Close inspection of Fig. 3A reveals the presence of an array of "micro-domains", or patches, ca 20-40Å in length and area ca 200-700Å^2. These islands exist on a background of large terraces, as before, with a height of ca 1.5Å above the regions surrounding each patch. (This height difference is responsible for the "lighter" shade of the microdomains in the STM images.) Occasionally, atomic-resolution images within each island could be obtained. One such image,

shown in Fig. 3B, shows clearly the presence of a (1 x 1) lattice, again with unit-cell dimensions (2.7-2.8Å) and row directions that match precisely that expected for the unreconstructed Pt(1CO) surface

Sweeping the potential in the positive direction yields significant changes in the microdomain morphology. Figure 3C shows an image of a similar surface region as in Fig. 3A, but after sweeping the potential from -0.25 V to 0 V vs SCE. Comparison between Figs. 3A and C shows that the islands have become more closely packed in some regions of the latter image. Quantitative intercomparison between these images was restricted by the difficulty in imaging precisely the same surface region during such potential excursions. However, examination of a number of images confirmed the greater average density of these islands towards more positive potentials. Further positive alterations in the potential prior to the onset of CO electrooxidation, at ca 0.2 V vs SCE, yield eventual coalescence of the islands. At potencials positive of CO electrooxidation, into the oxide formation region (above ca 0.7 V vs SCE), the surface becomes irreversibly roughened, displaying a multitude of "ball-like" features associated with oxide-induced surface disorder. These features, approximately 1-2 atomic diameters in height, are comparable to those observed in ref. 28.

Similar results to those in Fig. 3A-C were obtained irrespective of the precise conditions under which the adsorbed iodine was replaced by CO. Variants of the procedure included transferring the surface to the STM cell after I/CO replacement in the electrochemical pretreatment cell, and adding CO while the iodine-coated surface is potentiostated at more positive potentials, ca 0 to 0.1 V vs SCE. Under the last condition, replacement of adsorbed iodine by CO was sufficiently slow (~ few minutes) that the process could be following during subsequent STM imaging. Interestingly, the removal of the ordered iodine adlattice and its replacement by the CO-induced microdomains could be discerned as "wavefronts" creeping over portions of the (80 x 80 nm) STM image region.

Electrooxidative removal of the adsorbed CO, flushing with 0.1 M $HClO_4$ and readsorption of iodine from 1 mM iodide solution, yielded a partial reversion of the surface morphology in that larger, ca 50 nm, patches of a c($\sqrt{2}$ x $5\sqrt{2}$)R45° (θ_I = 0.6) adlayer are evident.

Given the observation of marked potential-dependent changes in surface morphology induced by adsorbed CO, it is of interest to perform parallel IRAS measurements so to provide information on the CO adlayer structure under these conditions. Figure 4 shows such a potential-dependent sequence of infrared spectra in the C-O stretching (ν_{co}) region, 1800-2150 cm^{-1}, obtained for a saturated CO adlayer on Pt(100) in CO-saturated 0.1 M $HClO_4$. The surface, pretreated using Method I, was transferred with the iodine adlayer intact to the spectroelectrochemical cell, where the iodine was replaced by CO at -0.25 V by CO sparging just prior to forming the spectral thin layer and acquiring the IRAS data. The results in Fig. 4 are similar to those reported previously, in Fig. 4A of ref. 17. At the initial potential, an intense ν_{co} band is observed at 2052 cm^{-1}, with a weaker feature at 1874 cm^{-1}, ascribed to terminal (atop) and twofold bridging CO, respectively. Sweeping the potential in the positive direction yields an attenuation of the bridging ν_{co} feature and a concomitant increase in the terminal ν_{co} band intensity, prior to electrooxidative CO removal at ca 0.3 V vs SCE. The fractional CO coverage, θ_{co}, present under the IRAS and STM conditions employed here is 0.85 (±0.05), as deduced from the absorbance of the 2343 cm^{-1} CO_2 band formed by electrooxidation of the adsorbed CO.[17]

DISCUSSION

The present STM results indicate that Pt(100) electrode surfaces prepared by flame annealing consist substantially of (1 x 1) domains, i.e., are largely unreconstructed, in the presence of saturated iodine or CO adlayers. This finding is consistent with extensive structural studies in uhv, especially using low energy electron diffraction (LEED), which as noted above show that the hex reconstruction is lifted entirely by CO and other adsorbates even at ambient

temperatures.[9,10] Reconstruction of the "clean" (1 x 1) Pt(100) surface to the thermodynamically more stable hex surface phase does not occur at temperatures below ca 400K.[10c] One therefore has good reason to anticipate that ordered Pt(100) electrodes prepared by procedures involving iodine and/or CO adsorption would consist largely of unreconstructed (1 x 1) domains, even following adsorbate removal.

More surprising, then, is the present finding that CO adsorption yields concentrated arrays of (1 x 1), presumably Pt substrate, domains of only limited dimensions, ca 20–40Å, surrounded presumably by "fault lines" or other topographically distinct features. Nevertheless, there is evidence from other sources that lend support to such qualitative characteristics of Pt(100) surfaces containing saturated ($\theta_{co} \approx 0.85$) CO adlayers. A LEED analysis of θ_{co}-dependent domain sizes for CO adsorption on Pt(100) in uhv shows that larger domains are formed at intermediate coverages starting from a (1 x 1) than for a "hex" surface, as expected since the adsorption process on the latter surface will entail substantial substrate structural rearrangement.[10a] [The formation of such domains upon CO adsorption on a hex Pt(100) surface in uhv has also been observed directly by STM.[11a]] Nonetheless, only small c(2 x 2) CO domains (containing 20 molecules or less) are formed even on the initially (1 x 1) surface at high CO coverages.[10a] Furthermore, a recent IRAS study in uhv has shown that a significant fraction of bridge-bound CO is present along with terminal CO on an initially (1 x 1) Pt(100) surface even at coverages, $\theta_{co} \approx 0.5$, where ($\sqrt{2}$ x $\sqrt{2}$)R45° domains are formed.[12a] Since these regions consist exclusively of terminal CO, the bridging CO appears to be present only at domain boundaries.[12a] It is worth mentioning in this context recent EELS data for the Pt(100)/CO system, which show that unlike the terminal CO, the bridging form exhibits only impact rather than dipole scattering.[29]

Given the potential-dependent form of the STM data in Fig. 3, the bridging CO band observed at ca 1875 cm^{-1} in the present IRAS spectra at the lower

potentials may well also arise from adsorbed CO present at the edges of the microdomains evident in the STM images. Supporting this notion is the observed attenuation of this feature at more positive potentials (Fig. 4) where some coalescence of the microdomains occurs. Still to be explained, however, is the underlying reason for the formation of smaller (1 x 1) substrate domains upon CO adsorption than are evident in the prior presence of iodine adlayers. Presumably the compressed CO adlayer obliges some substrate surface rearrangement, perhaps to accommodate the formation of bridging as well as terminal CO forms. As noted elsewhere,[18a,19] CO binding in bridging rather than terminal configurations is generally favored increasingly at lower potentials. The domain coalescence observed towards higher electrode potentials is consistent with the increasing energetic preference for (1 x 1) substrate domains containing almost exclusively terminal CO. The attenuation of bridging CO coordination on Pt(100) at more positive potentials has also been observed for surfaces prepared by flame annealing and water quenching.[30]

In conclusion, the present findings illustrate the virtues of atomic-resolution along with larger-scale STM images for providing detailed in-situ information on the substrate structure of monocrystalline metal electrodes susceptible to surface reconstruction. The value of combining potential-dependent STM data along with parallel adlayer structural information as provided by IRAS is also evident. We present elsewhere detailed information on potential-dependent reconstruction at low-index gold-aqueous interfaces obtained from atomic-resolution STM.[31] In-situ STM therefore seems destined to become a valuable tool for the atomic-level exploration of surface reconstruction in electrochemical, as well as uhv, systems.

ACKNOWLEDGMENTS

This work is supported by the Industrial Associates Program at Purdue University, funded in part by Dow Chemical Co. and BP America (to BCS), and by a grant from the National Science Foundation (to MJW).

REFERENCES AND NOTES

1. Yau, S.-L.; Vitus, C.M.; Schardt, B.C., J. Am. Chem. Soc., 1990, 112, 3677.

2. Magnussen, O.M.; Hotlos, J.; Nichols, R.J.; Kolb, D.M.; Behm, R.J., Phys. Rev. Lett., 1990, 64, 2929.

3. Yau, S.-L.; Gao, X.; Chang, S.-C.; Schardt, B.C.; Weaver, M.J., J. Am. Chem. Soc., 1991, 113, 6049.

4. Wiechers, J.; Twomey, T.; Kolb, D.M.; Behm, R.J., J. Electroanal. Chem., 1988, 248, 451.

5. Trevor, D.; Chidsey, C.E.D.; Loiacono, D.N., Phys. Rev. Lett., 1989, 62, 929.

6. Houbo, H.; Sugawara, S.; Itaya, K., Anal. Chem., 1990, 62, 2424.

7. For a recent review, see: Somorjai, G.A.; Van Hove, M.A., Prog. Surf. Sci., 1989, 30, 201.

8. Hagstrom, S.B.; Lyon, H.B.; Somorjai, G.A., Phys. Rev. Lett., 1965, 15, 491.

9. (a) Morgan, A.E.; Somorjai, G.A., J. Chem. Phys., 1969, 51, 3309; (b) Barteau, M.A.; Ko, E.I.; Madix, R.J., Surface Science, 1981, 102, 99; (c) Bonzel, H.P.; Pirug, G., Surface Science, 1977, 62, 45.

10. (a) Behm, R.J.; Thiel, P.A.; Norton, P.R.; Ertl, G., J. Chem. Phys., 1983, 78, 7437; (b) Thiel, P.A.; Behm, R.J.; Norton, P.R.; Ertl, G., J. Chem. Phys., 1983, 78, 7448; (c) Norton, P.R.; Davies, J.A.; Creber, D.K.; Sitter, C.W.; Jackman, T.E., Surface Science, 1981, 108, 205.

11. (a) Hösler, W.; Ritter, E.; Behm, R.J., Ber Bunsenges. Phys. Chem., 1986, 90, 205; (b) Ritter, E.; Behm, R.J.; Pötschke, G.; Wintterlin, J., Surface Science, 1987, 181, 403.

12. (a) Gardner, P.; Martin, R.; Tüshaus, M.; Bradshaw, A.M., J. Electron Spect. Related Phenom., 1990, 54/55, 619; (b) Gardner, P.; Tüshaus, M.; Martin, R.; Bradshaw, A.M., Surface Science, 1990, 240, 112.

13. (a) Clavilier, J.; Faure, R.; Guinet, G.; Durand, R., J. Electroanal. Chem., 1980, 107, 205; (b) Also see: Clavilier, J., ACS Symp. Ser., 1988, 378, 202.

14. Zurawski, D.; Rice, L.; Hourani, M.; Wieckowski. A., J. Electroanal. Chem., 1987, 230, 221.

15. Schardt, B.C.; Yau, S.-L.; Rinaldi, F., Science, 1989, 243, 1050.

16. (a) Yau, S.-L., Ph.D. thesis, Purdue University, 1990;
(b) Thiehsen, R., Ph.D. thesis, Purdue University, 1990;
(c) Vitus, C., Ph.D. thesis, Purdue University, 1991.

17. Chang, S.-C.; Weaver, M.J., J. Phys. Chem., 1990, 94, 5095.

18. For recent overviews, see: (a) Chang, S.-C.; Weaver, M.J., J. Phys. Chem., 1991, 95, 5391; (b) Chang, S.-C.; Roth, J.D.; Ho, Y.; Weaver, M.J., J. Electron. Spect. Related Phenom., 1990, 54/55, 1185.

19. Chang, S.-C.; Weaver, M.J., Surface Science, 1990, 238, 142.

20. (a) Leung, L.-W.H.; Wieckowski, A.; Weaver, M.J., J. Phys. Chem., 1988, 92, 6985; (b) Chang, S.-C.; Leung, L.-W.H.; Weaver, M.J., J. Phys. Chem., 1989, 93, 5341; (c) Chang, S.-C.; Weaver, M.J., J. Chem. Phys., 1990, 92, 4582; (d) Chang, S.-C.; Weaver, M.J., Surface Science, 1990, 230, 222.

21. (a) Leung, L.-W.H.; Chang, S.-C.; Weaver, M.J., J. Chem. Phys., 1989, 90, 7426; (b) Chang, S.-C.; Weaver, M.J., J. Electroanal. Chem., 1990, 285, 263.

22. (a) Chang, S.-C.; Weaver, M.J., Surface Science, 1991, 241, 11; (b) Chang, S.-C.; Roth, J.D.; Weaver, M.J., Surface Science, 1991, 244, 113.

23. Gao, X., et al, in preparation.

24. Schardt, B.C., unpublished work.

25. Chang, S.-C.; Yau, S.-L.; Schardt, B.C.; Weaver, M.J., J. Phys. Chem., 1991, 95, 4787.

26. Sawyer, D.T.; Roberts, J.L., Jr., "Experimental Electrochemistry for Chemists", Wiley, New York, 1974, p.39.

27. The iodine and CO coverages, θ_I and θ_{CO}, respectively, quoted here are defined (as is conventional) as the ratio of adsorbate atoms/molecules to the Pt atoms present on the unreconstructed (1 x 1) Pt(100) surface.

28. Itaya, K.; Sugawara, S.; Sashikata, K.; Furuya, N., J. Vac. Sci. Technol., 1990, A8, 515.

29. Kizhakevariam, N.; Stuve, E., in preparation.

30. (a) Watanabe, S.; Kinomoto, Y.; Kitamura, F.; Takahashi, M.; Ito, M., J. Electron Spect. Related Phenom., 1990, 54/55, 1205; (b) Kitamura, F.; Takahashi, M.; Ito, M., J. Phys. Chem., 1988, 92, 3320.

31. Gao, X.; Hamelin, A.; Weaver, M.J., Phys. Rev. Lett., 1991, 67, 618.

FIGURE CAPTIONS

Fig. 1

Unfiltered atomic-resolution STM image of c($\sqrt{2}$ x 5$\sqrt{2}$)R45°-I adlayer, prepared by Method I (see text), on Pt(100) in 0.1 M $HClO_4$ at 0.25 V vs SCE. Imaging conditions: V_b = -35 mV, i_t = 5.0 nA; "constant height" mode.

Fig. 2

Atomic-resolution STM image of Pt(100) substrate in air, for surface prepared by Method II with iodine adlayer adsorbed from 1 mM KI + 0.1 M $HClO_4$. Tunneling conditions: V_b = 50 mV, i_t = 15 nA; "constant height" mode.

Fig. 3A

STM image of Pt(100) in 0.1 M $HClO_4$ containing near-saturated CO, at -0.25 V vs SCE. Surface was prepared by Method I, with iodine adlayer replaced by CO at -0.25 V within STM cell (see text). Imaging conditions: V_b = -65 mV, i_t = 3.0 nA; "constant current" mode.

Fig. 3B

Atomic-resolution STM image of Pt(100) in 0.1 M $HClO_4$ near-saturated CO at -0.25 V vs SCE under conditions similar to Fig. 3A. Imaging conditions: V_b = 150 mV, i_t = 3.0 nA; "constant current" mode.

Fig. 3C

As in Fig. 3A, but after sweeping electrode potential to 0 V vs SCE. Imaging conditions: V_b = -65 mV, i_t = 1.0 nA; "constant current" mode.

Fig. 4

Potential-dependent sequence of infrared absorbance spectra in 1800-2150 cm^{-1} frequency region for CO adsorbed on Pt(100) in 0.1 M $HClO_4$ containing saturated (ca 1 mM) CO. Surface prepared by using similar procedure to that in Fig. 3A. Spectra acquired during 1 mV s^{-1} positive-going potential sweep from -0.25 V vs SCE. Each spectrum entailed acquiring 100 interferometer scans, subtracted from which was a similar set obtained following complete CO electrooxidation (at 0.5 V) so to remove solvent interferences. Potentials indicated beside each spectrum are average values (vs SCE) during data acquisition (see ref. 17 for further details).

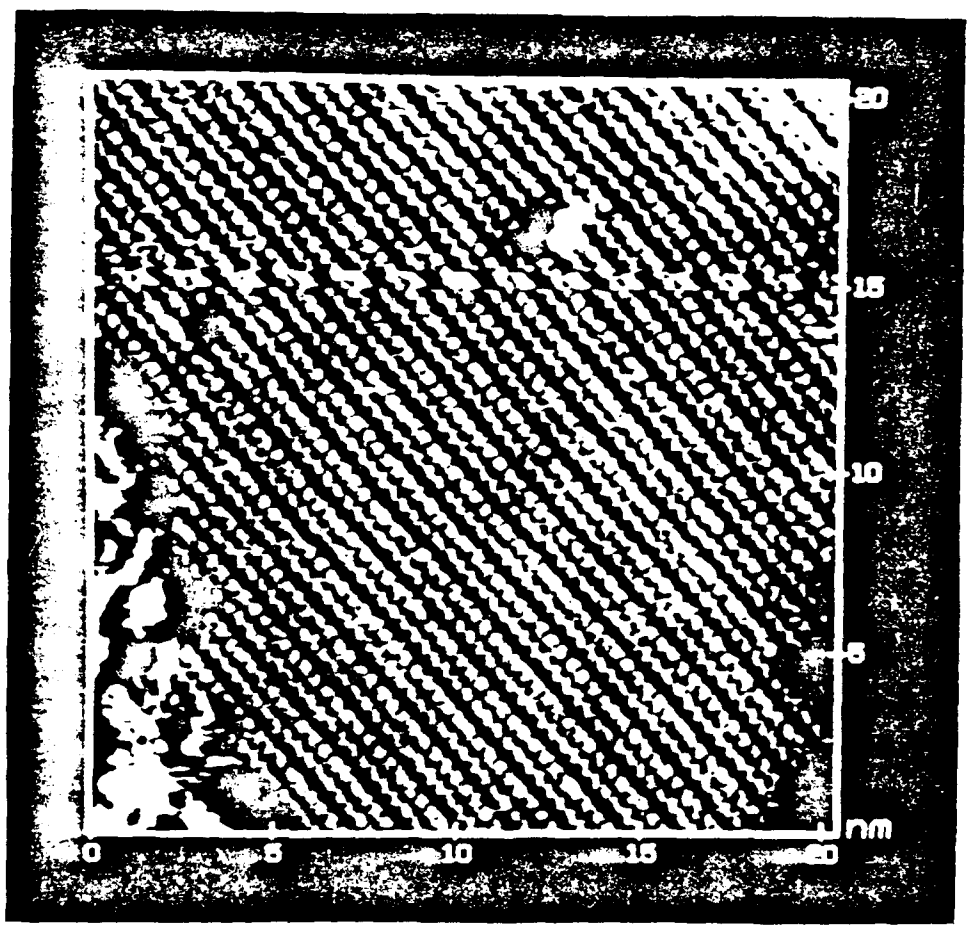

FIG 1

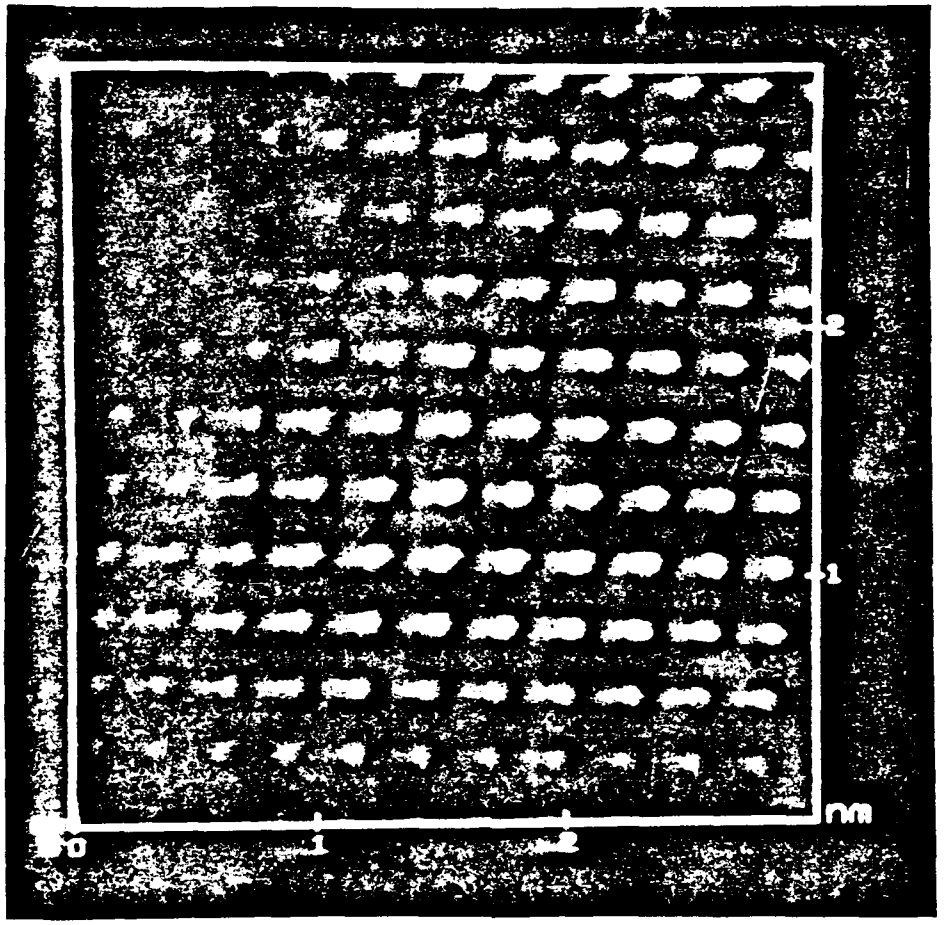

FIG 2

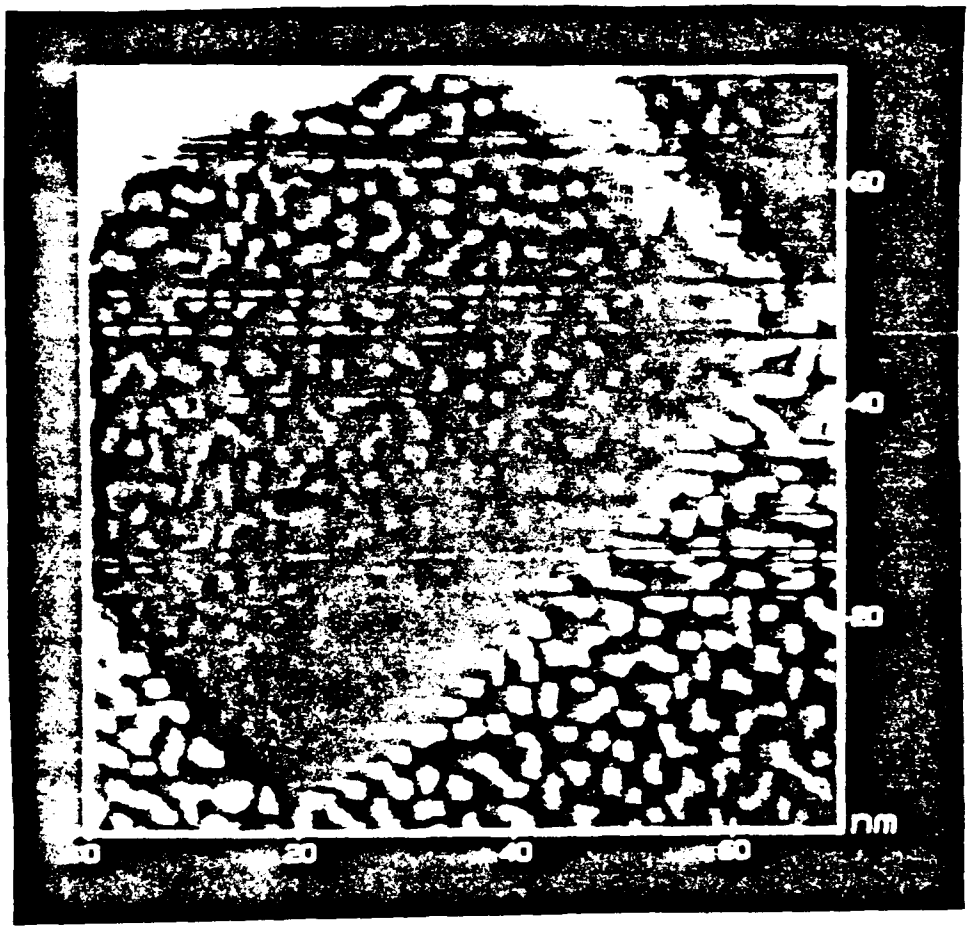

FIG 3A

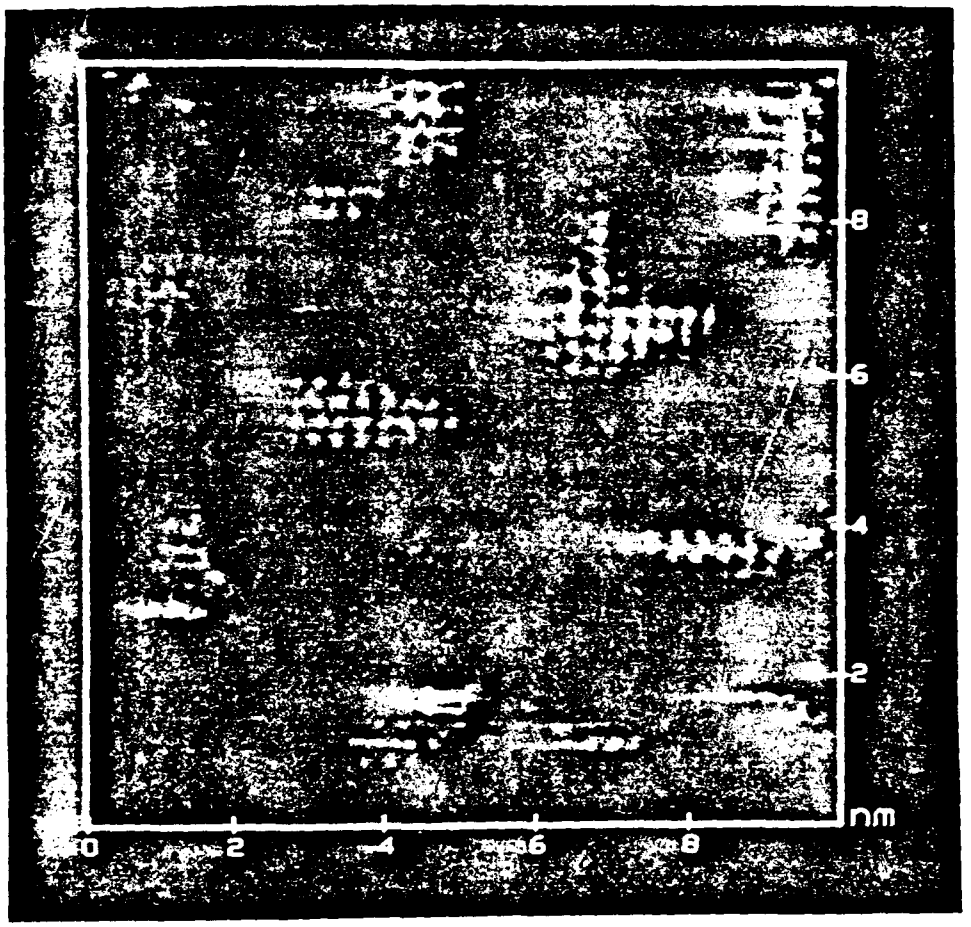

FIG 3B

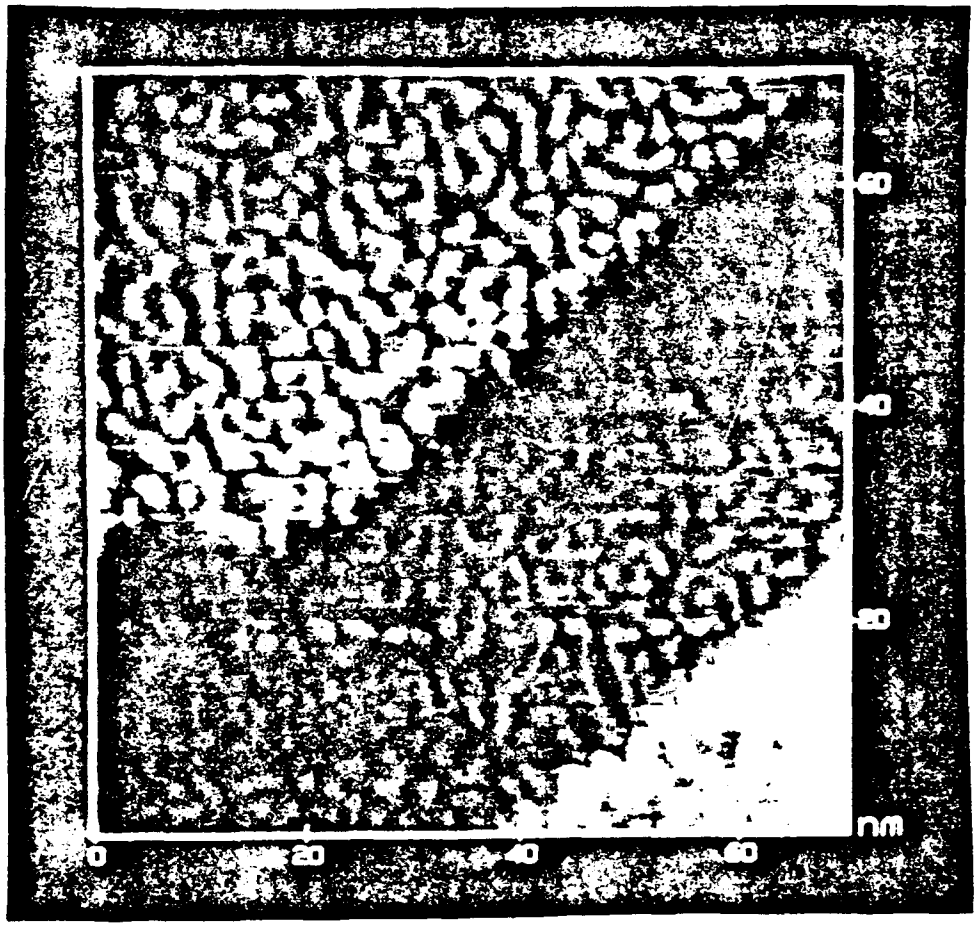

FIG 3C

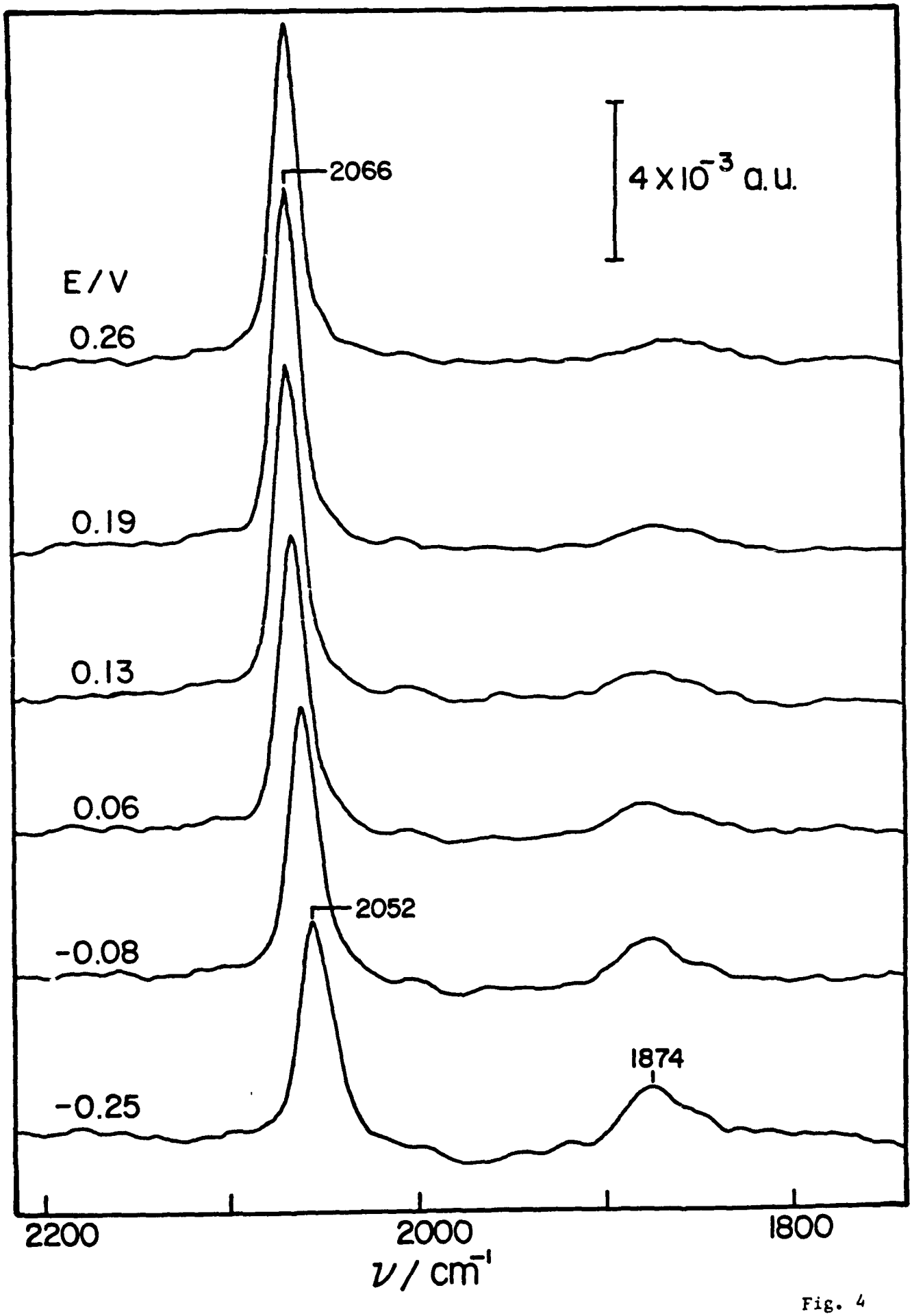
2066
4 X 10⁻³ a.u.
E / V
0.26
0.19
0.13
0.06
-0.08
-0.25
2052
1874
2200
2000
1800
ν / cm⁻¹

Fig. 4